

THE CASE OF AN INTEGRATED GLOBAL HYDROSPHERE ON EARLY MARS: CLUES FROM THE DISTRIBUTION OF ANCIENT DELTAS AND VALLEY NETWORKS. Gaetano Di Achille¹ and Brian M. Hynek^{1,2}, ¹Laboratory for Atmospheric and Space Physics, University of Colorado, 392 UCB, Boulder, CO 80309, United States, ²Department of Geological Sciences, University of Colorado, 399 UCB, CO 80309, United States.

Introduction: The climate of early Mars could have supported a global hydrological system [1], cycling water across the planet by integrating precipitation, groundwater reservoirs, ice accumulation regions, and surface runoff toward lakes, seas, and possibly a northern hemispheric ocean [1-5]. Here we use co-registered global database of currently known martian deltaic deposits [e.g., 6, 7, 8] and valley networks [9] in conjunction with the topography from Mars Observer Laser Altimeter (MOLA) data [10] for testing the occurrence of an integrated global hydrosphere and of a northern hemispheric ocean on early Mars.

Rationale: Deltas are among the most typical coastal landforms on Earth. They form ideally at the same elevation all over the planet (the mean global sea level), which is approximated by the geoid. Analyses of terrestrial deltas and their worldwide correlation have given clues on global trends and changes of the mean sea level during the geological history of the Earth [11]. In agreement with the terrestrial paradigm, the planetwide correlation of the current absolute elevation of martian deltas can be used as a proxy for the past mean global sea level of Mars, assuming that (i) the present topography is a reasonable representation of that at the time of the putative ocean (as supported by [12]), and that (ii) the deltaic deposits formed during the same epoch of sustained global hydrological activity (as supported by [7, 9, 13, 14]). Potentially, this analysis also gives clues on any global groundwater aquifer possibly saturating the crust and systematically emerging on the surface of the planet [5].

Methods: The elevation values of the apex (maximum water level), delta front (mean highstand), and of the basin floor (minimum water level) were extracted for each delta. These morphometric indicators were plotted as function of longitude (Fig. 1) to detect possible equipotential surfaces indicative of ancient ocean coastlines. Additionally, we extracted the termini elevations of all the valleys [9], in order to compare them with the distribution of deltas (Fig. 2). In fact, if a planetwide body of water was present when the deltas were forming, then it should have determined abrupt channel terminations all over the planet at approximately the same elevation indicated by the analysis of the deltas.

Results: The highstand levels of all 52 deltaic deposits show a mean value of about -1848 m ($\sigma = 1126$

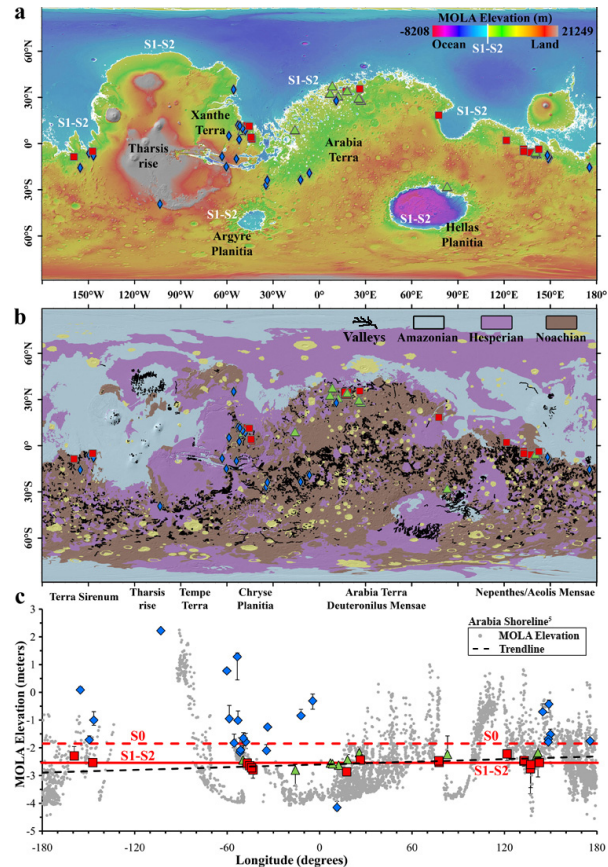


Figure 1. a) MOLA map with superimposed deltas; white contours indicate S1 and S2. **b)** Map of martian valley networks (black lines, [9]) and relationships with the three major geological epochs [16, 17]. **c)** Plot of the deltas' indicators as function of longitude.

m (herein referred to as S0). Whereas, 17 of the deltas are not contained in a basin or were formed in basins or outflow channels that connect to the northern lowlands (~33% of total, red squares in Fig. 1). These delta front elevations define the best approximation of an equipotential surface (herein referred to as S1) at the mean elevation of -2540 m ($\sigma = 177$ m, Fig. 1). Indeed, a contour traced at this elevation effectively outlines a complete closure within and along the margins of the northern lowlands, encompassing the boundary of the basin within which the deposits formed (Fig. 1a-c and 3a). Moreover, S1 is consistent with large portions of the "Arabia shoreline" previously identified from geomorphologic and topographic analyses [3, 4, 5] (Fig. 1c and 3a) and is close to its

average value (-2499 m, compare the trendline of this contact with the **S1** surface in Fig. 1c). The second closest approximation of a surface of equal gravitational potential (herein referred to as **S2**) is found at -2482 m ($\sigma = 200$ m) by considering an additional twelve deltas formed in closed basins (green triangles in Fig. 1), totaling ~55% of the current global database. However, since this has been inferred by considering also deltas formed in closed basins, it implies that a water table should have approximately intersected the surface at this base level all over the planet. Indeed, the **S2** level is remarkably close to the -2550 m level suggested by theoretical calculations for the global distribution of water during the Noachian [5]. The latter value, in fact, was derived from thermophysical properties of Mars with the assumption that water was saturating the crust and ponding in hydrostatic equilibrium on the surface of the planet [5]. Therefore, the present analysis supports the latter thermal-hydraulic reconstruction, implying that a vast ocean and large seas were present in the northern hemisphere and in Argyre and Hellas basins, respectively. Several groundwater-fed paleolakes would have also contemporarily emerged within a few hundreds of kilometers-wide region upslope from the **S2** ocean boundaries and the crustal dichotomy and around the rim of Argyre and Hellas within craters deep enough to reach the **S2** level (Fig. 1a and 3a). Both the latter equipotential surfaces (**S1-S2**) are also generally consistent with the distribution of valley networks (Fig. 2) at a global scale: (i) the majority of the valleys terminate at higher elevation with respect to the inferred levels, (ii) a particularly good match between **S1-S2** and terminations of valleys is found at Terra Sirenum and Aeolis/Nepenthes Mensae regions, (iii) less than 1% of Noachian valleys are located at lower elevations, and finally (iv), 12-16% of Hesperian and Amazonian valleys, show terminations below the **S1-S2** levels (Fig. 2), likely suggesting a progressive retreat of the ocean after its maximum extension during the Late Noachian.

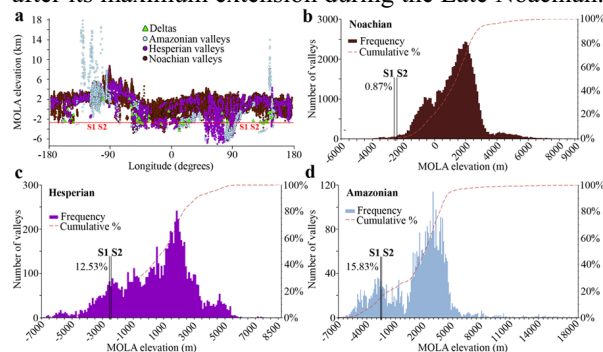


Figure 2. a, Elevations of valleys and deltas as function of longitude. The red line shows **S1** and **S2**. **b, c, d,** Histograms showing the distribution of Noachian, Hesperian, and Amazonian valleys vs. MOLA.

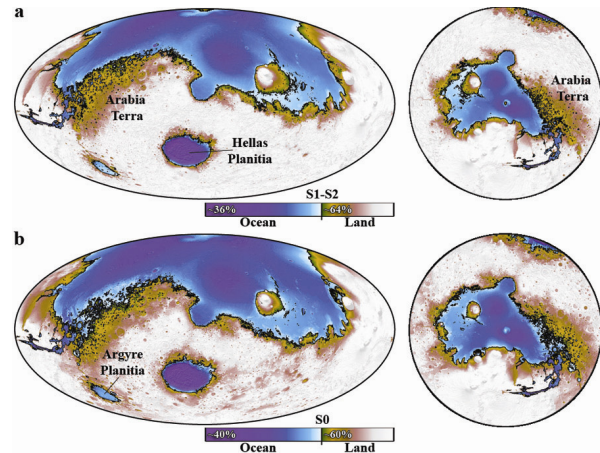


Figure 3. Hammer (left) and north polar stereographic (right) projections from MOLA showing the enclosures (black lines) defined by **S1-S2** (a) and **S0** (b).

Furthermore, the distribution and outlet elevation of the 210 known martian paleolakes within open basins [15] are also consistent with the elevation of the **S1-S2** enclosures: a negligible amount of lake outlets shows terminations below these levels [15].

Conclusions: **S1** and **S2** are broadly consistent with paleoshorelines independently suggested based both on morphologic, topographic, and thermophysical considerations, and with the global distribution of valley networks. These results support existing theories regarding the extent and formation time of an ancient martian ocean. Given the key assumptions of this analysis, the inferred boundaries likely reflect the maximum extension of a global hydrosphere near the Noachian-Hesperian boundary. However, the almost total lack of deltaic deposits below the inferred levels seems to exclude the occurrence of Hesperian-Amazonian oceans within the northern plains, substantiating the notion that, after the end of the Noachian, overall climatic conditions were likely no longer supportive of sustained and widespread hydrological activity.

References: [1] Baker et al. (1991) *Nature*, 352. [2] Baker (2001) *Nature*, 412. [3] Parker et al. (1989) *Icarus*, 82. [4] Parker et al. (1993) *J. Geophys. Res.*, 98. [5] Clifford and Parker (2001) *Icarus*, 154. [6] Malin and Edgett (2003) *Science*, 302. [7] Irwin et al. (2005) *J. Geophys. Res.*, 110. [8] Di Achille et al. (2009) *Geophys. Res. Lett.*, 36. [9] Hynek et al. (2009) *J. Geophys. Res.*, submitted. [10] Smith et al. (2001) *J. Geophys. Res.*, 106. [11] Stanley and Warne (1994) *Science*, 265. [12] Phillips et al. (2001) *Science*, 291. [13] Howard et al. (2005) *J. Geophys. Res.*, 110. [14] Fassett and Head (2008) *Icarus*, 195. [15] Fassett and Head (2008) *Icarus*, 198. [16] Scott and Tanaka (1986) *USGS Map, I-1802-A*. [17] Greeley and Guest (1987) *USGS Map, I-1802-B*.